SUPPORTING INFORMATION

SI MATERIALS AND METHODS

Assembly of dual-luciferase reporters

For comparison with the *lpp* leader we used a synthetic RBS Ec-TTL-R0004, from here on denoted as "5′UTR$_{R0004}$" (1). Dual luciferase vectors used for *in vivo* experiments (i.e., dl_*lpp* and dl_*R0004*; **Fig. S1B,C**) were generated through three-segment Gibson assembly (2). First, p00094 vector, a pET24a-based vector expressing a monocistronic mRNA containing the 5′UTR of the pET24a followed by the Firefly and Renilla luciferase genes (*fluc* and *rluc*, respectively), was linearized using the oligonucleotide pairs pET_F/pET_R and pET_F /pET_WR (**Table S1**). The PCR-linearization of the vector gave as products two amplicons, pET_*lpp* and pET_*R0004*, of 5167 and 5168 bp, respectively. Second, the DNA-portion containing the *fluc* gene preceded by the pET24a 5′UTR (p00094) and common to both dual-luciferase expression vectors (**Fig. S1B**) was PCR-amplified using the oligonucleotide pair Fluc_F/Fluc_R (**Table S1**). The resulted amplicon (pET_*fluc*) is 1724 bp in size and overlaps at one end with one side of the two previously obtained linearized vectors (i.e., pET_*lpp* and pET_*R0004*), whereas at the opposite side overlaps with fragments *rluc_lpp* and *rluc_R0004* (see below). *rluc_R0004* amplicon (976 bp) was obtained by PCR amplification of *rluc* gene using the oligo pair Rluc_WF/Rluc_R (**Table S1**). To allow transcription from the T7 promoter the original sequence of Ec-TTLR004 was modified by addition of one G at the 5′-end of the 5′UTR$_{R0004}$ (5′-gTCTAGAGAAAGATTAGAGTCACCAT-3′). On the other hand, the *rluc_lpp* amplicon (987 bp), containing the 5′UTR of the *lpp* gene and the *rluc* coding sequence, was obtained via two consecutive amplifications steps. Rluc_F1/Rluc_R (**Table S1**) oligo pair was first used to obtain *rluc_lpp_F1* fragment (970 bp), which was then used as template in the following PCR amplification using oligo pair Rluc_F/Rluc_R (**Table S1**). The three-segment Gibson assembly reactions contain overlapping regions of 50-60 bp and were performed as recommended by the manufacturer (New England Biolabs). Assembly of pET_*lpp*, pET_*fluc* and *rluc_lpp* amplicons led to circular vector dl_*lpp* (7813 bp; **Fig. S1B**). Assembly of pET_R0004, pET_*fluc* and *rluc_R0004* amplicons led to a circular vector dl_*R0004* (7801 bp; **Fig. S1B**). Both vectors have as internal control the *fluc* coding sequence preceded by the highly expressed 5′UTR built-in the pET24a vector. Upstream the polycistronic mRNA is the *rluc* coding

sequence which is in one case preceded by the 5′UTR of *lpp* mRNA (dl_*lpp*) and in the other case by the 5′UTR$_{R0004}$ (dl_*R0004*). In both cases the polycistronic mRNA is under the control of the T7 promoter. Newly assembled vectors were sequenced to confirm the correct assembly.

Dual luciferase assay

Individual aliquots of Tuner(DE3) chemically competent cells were transformed with the dual luciferase vectors (i.e dl_*lpp* and dl_*R0004*). Isolated transformants were grown to an OD_{600} of 0.5 and the expression of the polycistronic mRNA was induced with 100 µM of IPTG. After 30 minutes from the IPTG addition 100 µl aliquots were removed from each flask, cells were pelleted and supernatant discarded. Cell pellets were first washed with 200 µl 0.9 % of NaCl and then resuspended with 0.9 % NaCl to a final concentration of 2 mOD_{600} per µl. Cells were lysed by addition of an equal volume of 2X lysis buffer (pjk GmbH) followed by 10 min incubation on ice. Lysates were clarified by centrifugation and immediately flash-frozen in liquid nitrogen. Prior to performing luciferase assays each frozen lysate aliquot was incubated 5 minutes at 37 °C. Firefly luciferase assay was performed by mixing 4 µl of cell lysate with 90 µl of Beetle-Juice supplemented with D-luciferin and ATP according to manufacturer guidelines (pjk GmbH), followed by 5 min incubation at 25 °C. Analogously, Renilla luciferase activity was performed by mixing 4 µl of cell lysates with 90 µl of Renilla Glow-Juice supplemented with coelenterazine (see manufacturer guidelines; PJK GmbH), followed by 5 min incubation at 25°C. The activities of Firefly and Renilla luciferases were measured using the same delay and integration time (i.e. 2 and 4 s, respectively) in a Sirius luminometer (Berthold).

Preparation of mRNA. The 5**lpp* 5'UTR was used as a primer for poly(U) synthesis using a template-independent poly(U)-polymerase (New England Biolabs). Reactions were carried out according to the manufacturer's protocol, except for the addition of $MgCl_2$ (7 mM) and RNase inhibitor (1.6 units/µl) (RiboLock, Fermentas). The RNA primers (*lpp* UTR or *lpp*$_{AUU}$ UTR) used in the extension reactions were purchased from IBA (Göttingen), and were either unlabeled or labeled with a Atto488 at the 5' end. The RNA primers were heated for 2 min at 95°C in H_20 and DMSO (20%) before adding to reactions. Extension reactions were carried out for 30 min at 37°C, and the mRNA was purified using the RNeasy Midi Kit columns (Qiagen). Before use, mRNAs were re-folded by incubation in water for 1 min at 90°C, cooled on ice for 1 min, and then incubated in buffer A (50 mM Tris-HCl, pH 7.5, 70 mM NH_4Cl, 30 mM KCl, 7 mM $MgCl_2$) at 37°C for 20

min. The full-length *lpp* mRNA was amplified by PCR from the genome of *E. coli* BL21DE3 with the help of the following primers:
forward GGCCAGTGTAATACGACTCACTATAGCTACATGGAGATTAACTCAATC; and reverse CATGATTACGCCAGTAGCGGTAAACGGCAGAC. The amplified fragment was cloned into a pUC19 plasmid with the help of Gibson assembly mixture (3). The purified DNA template was used for the T7 RNA-polymerase transcription. DNA template (0.05 μM), T7 RNA-polymerase (1.6 units/μl), pyrophosphatase (0.01 units/μl), RNase inhibitor (0.2 units/μl), $MgCl_2$ (3.5 mM), DTT (10 mM), and GMPγS (10 mM) GTP (1 mM) ATP (3 mM), CTP (3 mM), and UTP (3 mM) were incubated in the transcription buffer (40 mM Tris-HCl pH 7.5, 15 mM $MgCl_2$, 2 mM spermidine, 10 mM NaCl) for 4 h at 37°C and the mRNA purified by HiTrap 5 ml column (GE Healthcare) on Äkta Purifier Plus. The mRNA was fluorescence labeled in phosphate buffer (0.1 M), pH 7.2, using a 50-fold molar excess of the ATTO488 maleimide over the mRNA for 2 h at room temperature. The reaction was stopped by ethanol precipitation and the mRNA purified by HiTrap Q HP 5 ml column (GE Healthcare). The length and homogeneity of all the mRNAs products were assessed by PAGE on denaturing gels containing urea (Fig. S1E, F and Fig.S5A).

Initiation and translation assays. All reactions were performed in buffer A at 37°C; in stopped-flow experiments, 1 mM DTT was added. Ribosomes from *E. coli* MRE 600, initiation factors (IF1, IF2, IF3), f[^{3}H]Met-tRNA^{fMet}, [^{14}C]Phe-tRNA^{Phe}, EF-Tu, and EF-G were prepared as described (4-9). The rpsB1 mutation was introduced into the chromosome-encoded rpsB (ribosomal protein uS2) gene in *E. coli* strain MDS57 (10) (courtesy of Michael Pearson, MPI for Biophysical Chemistry, Göttingen). The genomic region containing the mutant uS2 gene was PCR amplified from strain rpsB1 (11) using primers GGTATTGGTAGTCCCACAACACCGTAAGTGCCGTCAATGGTATCAC and GTCTATTGAATCGGAGCACCCACAGTCTTTCCTGAGACTGTCAACGAT. The plasmid pKO3 (12) was PCR amplified with primers ACTGTGGGTGCTCCGATTCAATAGACGGATCCTCTAGAGTCGACCGGAGA and TACGGTGTTGTGGGACTACCAATACCGCGGCCGCGATCCCCGGGTACCGA. The two PCR products were assembled into a circular plasmid using Gibson assembly (3), and the scarless genomic modification was generated by two-step homologous recombination generating strain MDP_130. The uS2 gene was sequenced using primers TGGGATACGTGGAGGCATAA and CGGTCACTTACTGATGTAAGCTC and the mutation determined to be a G to A transition

changing glutamate 170 to lysine (E170K). 30S subunit lacking proteins S1 and S2 were purified using established ribosome purification protocols (13). The relative stoichiometry of ribosomal proteins was determined by label-free quantitative mass spectrometry (Fig. S1K). In brief, wt and 70Δ ribosomes were treated with iodoacetamide and proteolyzed with trypsin as described (14). Peptides were analyzed by LC-ESI MS/MS in the data-dependent mode on a Q Exactive HF (Thermo Fisher) mass spectrometer. Thermo RAW files were processed with MaxQuant (1.5.5.1) using a Uniprot *E. coli* K12 database. Ribosomal proteins were quantified by intensity-based label-free quantification using MaxQuant Label Free Quantification (LFQ) values (15). The ratios of 70Δ and wild type ribosomes were normalized by the median ratio of all ribosomal proteins excluding S1 and S2.

To prepare 70S IC, a reaction mixture (1.5 ml) containing 70S (1 µM), mRNA (2 µM), f[^{3}H]Met-tRNA^{fMet} (3 µM), IF1, IF2 and IF3 (2 µM each) and GTP (0.5 mM) was incubated in buffer A for 30 min at 37°C. The 70S IC was purified by centrifugation through a sucrose cushion (1.1 M) in buffer A in a TLS 55 rotor (Beckman Coulter) for 2 h, 55,000 rpm at 4°C. The pelleted 70S IC was resuspended in buffer A, flash-frozen in liquid nitrogen and stored in aliquots at -80°C. The EF-Tu–GTP–Phe-tRNA^{Phe} ternary complex was prepared by incubating EF-Tu (2.5 molar excess over the Phe-tRNA^{Phe}), DTT (2 mM), GTP (2 mM), phosphoenolpyruvate (3 mM) (Roche), pyruvate kinase (0.1 mg/ml) (Roche) in buffer A for 15 min at 37°C. Subsequently, Phe-tRNA^{Phe} (4 µM) was added and the mix incubated for 2 min at 37°C before the start of the experiment. The elongation mixture was prepared by mixing ternary complexes with EF-G (4 µM).

The initiation efficiency was measured by nitrocellulose filter binding assay (**Fig. S1)**. Wild-type or mutant (lacking proteins S1/S2) 70S ribosomes (0.15 µM) or 30S subunit (0.15 µM), f[^{3}H]Met-tRNA^{fMet} (0.45 µM), initiation factors IF1, IF2 and IF3 (0.3 µM each) and GTP (0.5 mM) were incubated with mRNAs (0.45 µM). After incubation 50 µl aliquots were applied on nitrocellulose filters with 45µm pore size (Sartorius, Göttingen) and the filters were washed with cold buffer A. Filters were dissolved in 10 ml liquid scintillation cocktail (Quickszint 361; Zinsser Analytic) and the radioactivity on the filter was measured using a TriCarb counter (Perkin Elmer). The efficiency of 70S IC or 30S IC formation was estimated as the molar ratio between f[^{3}H]Met-tRNA^{fMet} and ribosomes in each aliquot.

To monitor the initiation on the free mRNA, 30S subunits were activated in buffer A containing 21 mM $MgCl_2$ for 20 min at 37°C and mixed with a 2-fold molar excess of IF1, IF2 and IF3, GTP (0.5 mM); when 30S IC formation was monitored, fMet-tRNA^{fMet} in 3-fold molar excess was

added. The components were incubated further for 20-30 min at 37°C. The mixture containing 30S subunits, IF1, IF2, IF3, and GTP was rapidly mixed in a stopped-flow apparatus (Applied Photophysics) with increasing concentrations of 5**lpp* mRNA (0.15 – 0.5 μM). For initiation of the second 30S subunit, purified 70S IC programmed with 5**lpp* mRNA (0.05 μM) were rapidly mixed with the elongation machinery and the 30S PIC as indicated in the figure legends.

Rapid kinetic measurements. To measure the rate of poly(Phe) synthesis, the experiments were performed using a quench-flow machine (KinTek Laboratories, Inc.) as follows. We mixed equal volumes of 70S IC (0.15 μM) containing 5**lpp* mRNA and f[^{3}H]Met-tRNA^{fMet} and of the elongation mixture (see above). At each time point the reaction was quenched with 0.5 M KOH, incubated for 30 min at 37°C and peptides were precipitated with trichloroacetic acid (TCA) (10%). The incorporated radioactivity was assessed by scintillation counting of f[^{3}H]Met and [^{14}C]Phe. After background correction the ratio between [^{14}C]Phe/f[^{3}H]Met was plotted against time. Data were analyzed by one-exponential fitting using Prism (GraphPad, San Diego, CA). To calculate the average elongation rate per amino acid, this value was multiplied by the synthesized peptide length. Error bars represent s.d. (n=4 independent experiments).

Stopped-flow experiments were performed using a SX-20MV apparatus (Applied Photophysics, Leatherhead, UK). The Atto 488 fluorophore at the 5'-end of the mRNA was excited at 465 nm and the emission was monitored after passing through a KV500 cut-off filter. Time courses were analyzed by one- or two-exponential fitting using Prism software. Standard errors were calculated from fitting the average derived from 7–10 time courses for each reaction. Lifetime values (τ) for time courses were calculated either as $\tau = 1/k$ for the cases where one-exponential fitting was sufficient or as $\tau = 1/(k_{app1}*A1+k_{app2}*A2)$ for two-exponential fitting, where A_1 and A_2 are fractions of the respective phases in the overall reaction amplitude. Errors are s.e.m. calculated from the s.e.m. values of the four fitting parameters. Elemental rate constants of the 30S PIC binding to the free mRNA were calculated from the apparent rate constants (k_{app1} and k_{app2}) at different 30S PIC concentrations using established analytical solutions (16). The concentration dependencies of the sum (Σ) and the product (Π) of k_{app1} and k_{app2} were evaluated by linear fitting and the elemental rates k_1, k_{-1}, k_2, k_{-2} were calculated from the slope and Y-axis intercept according to the following equations: slope $\Sigma = k_1$; intercept $\Sigma = k_{-1}+k_2 + k_{-2}$; slope $\Pi = k_1*(k_2 + k_{-2})$; intercept $\Pi = k_{-1}*k_{-2}$ (16). Errors are s.e.m. of the fit.

Global fitting of deconvoluted time courses. For deconvolution we used one original time course and one idealized time course (with the highest r^2 value) produced using built-in equations in Table Curve Software (Jandel Scientific). We subtracted the idealized time course from the respective experimental one to obtain the deconvoluted time course of fluorescence changes. We added the value of 1 or 2 to the fluorescence of each time point of the deconvoluted signal to avoid negative fluorescence values, which would otherwise impair the global fitting. The deconvoluted time courses obtained with two concentrations of 30S PIC (0.05 and 0.4 μM) were analyzed together by KinTek Explorer (17) using a global kinetic model containing four steps. Errors are s.e.m. of the fit at a threshold $\chi^2 = 0.99$.

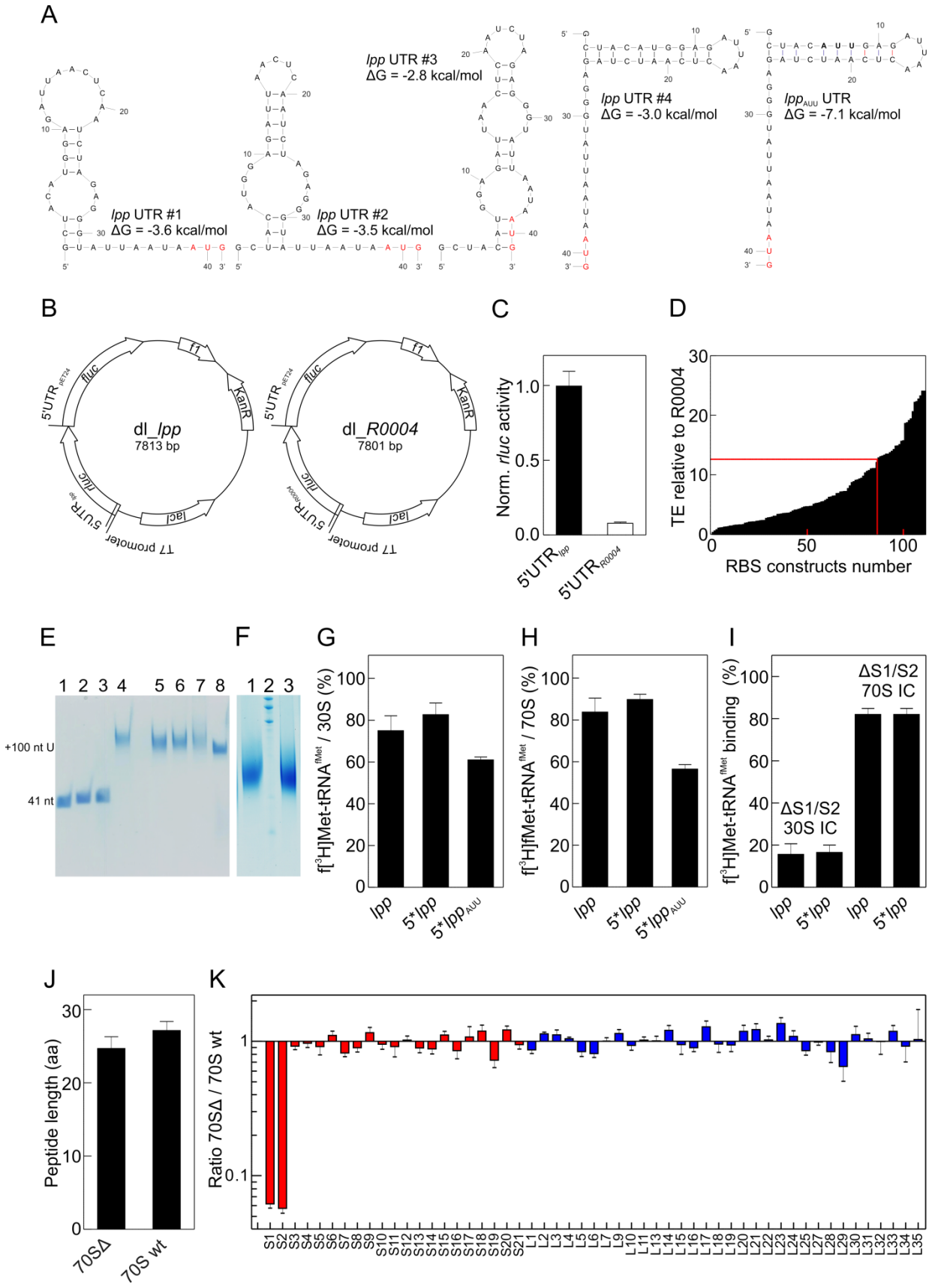
A
lpp UTR #1
ΔG = -3.6 kcal/mol
lpp UTR #2
ΔG = -3.5 kcal/mol
lpp UTR #3
ΔG = -2.8 kcal/mol
lpp UTR #4
ΔG = -3.0 kcal/mol
lpp AUU UTR
ΔG = -7.1 kcal/mol
B
dl_lpp
7813 bp
dl_R0004
7801 bp
f1
fluc
KanR
lac
T7 promoter
C
Norm. rluc activity
5'UTR lpp
5'UTR R0004
D
TE relative to R0004
RBS constructs number
E
+100 nt U
41 nt
F
G
f[3H]Met-tRNA fMet / 30S (%)
lpp
5*lpp
5*lpp AUU
H
f[3H]fMet-tRNA fMet / 70S (%)
I
f[3H]Met-tRNA fMet binding (%)
ΔS1/S2
70S IC
ΔS1/S2
30S IC
J
Peptide length (aa)
70SΔ
70S wt
K
Ratio 70SΔ / 70S wt

Fig. S1. Characterization of mRNA constructs and mutant ribosomes. (*A*) Putative secondary structures of the free 5'UTR of *lpp* mRNA predicted by Mfold (18). (*B*) Schematic representation of the dual luciferase reporters assembled to test the activity of different 5′UTRs. In both vectors the T7 expression leads to the transcription of a polycistronic mRNA. (*C*) Firefly (*fluc*) and Renilla (*rluc*) luciferase activity was measured upon 30 min expression with 100 μM IPTG (OD_{600} at the time of expression is 0.5, see Methods). Equal amount of cells were used in each assay. *Rluc* activity was measured in cells carrying either *dl_lpp* (black bar) or *dl_R0004* (white bar) and normalized by the respective *fluc* activity. Bars represent the mean of four individual experiments, error bars are s.d. (*D*) *In vivo* translation efficiency of 5'UTR_{lpp} shows a 12.6-fold higher expression of *lpp* with the respect of R0004 RBS (red line); only 24 of 111 constructs performed better (1). (*E*) Length and purity of the mRNAs. mRNAs were analysed on the 8% urea PAGE and visualized by methylene blue staining. Lanes 1-3, commercially purchased RNA oligo (*lpp*UTR) (20-30 pmol) without a reporter or labeled with Atto 540Q(5^{Q}*lpp*UTR) or Atto 488 (5**lpp*UTR). Lanes 4-7, mRNAs obtained by poly(U)-polymerase extension of the respective primers (20 pmol shown in lines 4-6, 10 pmol in line 7). Lane 8, the 101 nt-long mRNA used as a marker mRNA. (*F*) Comparison of the *lpp* (lane 1) and lpp_{AUU} mRNAs (lane 3) (30 pmol each) with a replacement of the potential start codon in the 5' UTR. Lane 2 is RNA ladder (408 nt, 350 nt, 240 nt). (*G*) 30S IC formation quantified by nitrocellulose filter binding experiments (Methods). (*H*) 70S IC formation quantified by nitrocellulose filtration. Same assay as in (*G*). Error bars represent s.e.m. calculated from 2 independent experiments. (*I*) Initiation efficiency on ribosomes lacking proteins S1 and S2. Same assay as in (*G* and *H*). Error bars represent s.e.m. calculated from 2 independent experiments. (*J*) Length of the peptide as translated by 70S wt and 70SΔ ribosomes. Error bars represent s.e.m. calculated from 2 independent experiments. (*K*) Relative stoichiometry of ribosomal proteins determined by quantitative mass spectrometry. Errors bars represent the standard deviation of three technical replicates with three independent LC-MS/MS runs each.

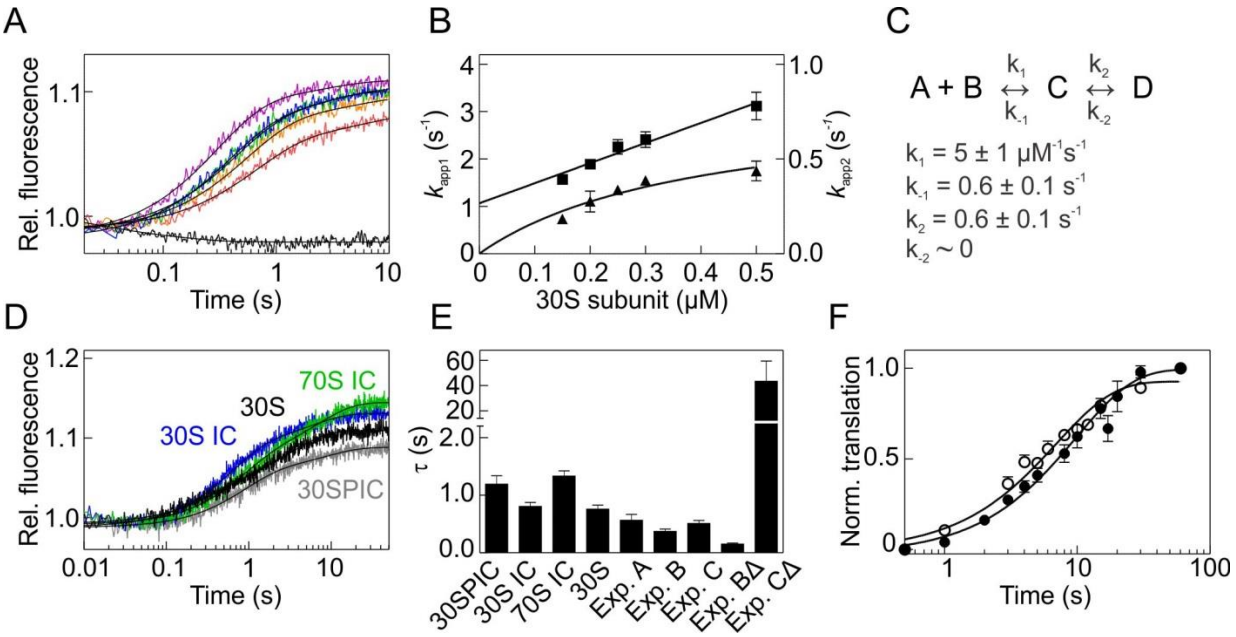

Fig. S2. Recruitment of the 30S subunit to the free 5**lpp* **mRNA.** (*A*) Time courses of binding at different 30S PIC concentrations. 30S subunits (0.15 μM, 0.2 μM, 0.25 μM, 0.3 μM and 0.5 μM) were incubated with IFs (1 μM) and GTP (0.5 mM) for 20 min at 37°C and mixed with a constant concentration of 5**lpp* mRNA (0.05 μM) in a stopped-flow apparatus. No fluorescence change occurred when the same reaction was carried out without the 30S subunit (black). Black lines show two-exponential fits, with the apparent rate constants k_{app1} and k_{app2}. (*B*) Concentration dependence of k_{app1} (squares) and k_{app2} (triangles). Error bars are s.e.m. from two independent experiments. Fitting was linear for k_{app1} and hyperbolic for k_{app2}, respectively. (*C*) The analysis of the elemental rate constants from the concentration dependencies shown in (*B*). The values are k_1 = 5 ± 1 μM^{-1} s^{-1} and k_{-1} = 0.6 ± 0.1 s^{-1}, k_2 = 0.6 ± 0.2 s^{-1}, and k_{-2} ~0 (with s.e.m. of the fit). (*D*) Time courses of the 30S (0.15 μM) recruitment to 5**lpp* mRNA in the presence of IF1, IF2, IF3 (0.3 μM), GTP (0.5 mM) in the presence of fMet-$tRNA^{fMet}$ (0.45 μM) and 50S subunit (0.15 μM) (70S IC, green trace) in the absence of the 50S subunit (blue trace), in the absence of both 50S subunit and $tRNA^{fMet}$ (gray trace) or in the absence of initiation factors, tRNA and 50S subunits (30S, black trace). Black lines show two-exponential fits. (*E*) Comparison of the average recruitment times (τ). Errors bars are s.e.m. (*F*) Normalized time courses of 5**lpp* translation with wild type 70S (closed circles) or with 70SΔ (open circles). Peptides were TCA precipitated and translation quantified as a ratio of [^{14}C]Phe pmol incorporated per pmol of f[^{3}H]Met. The average elongation rate per amino acid (k_{el}) is k_{el} = 2.8 ± 0.3 aa·s^{-1} and 2.4 ± 0.3 aa·s^{-1} for the wt 70S and 70SΔ ribosomes, respectively.

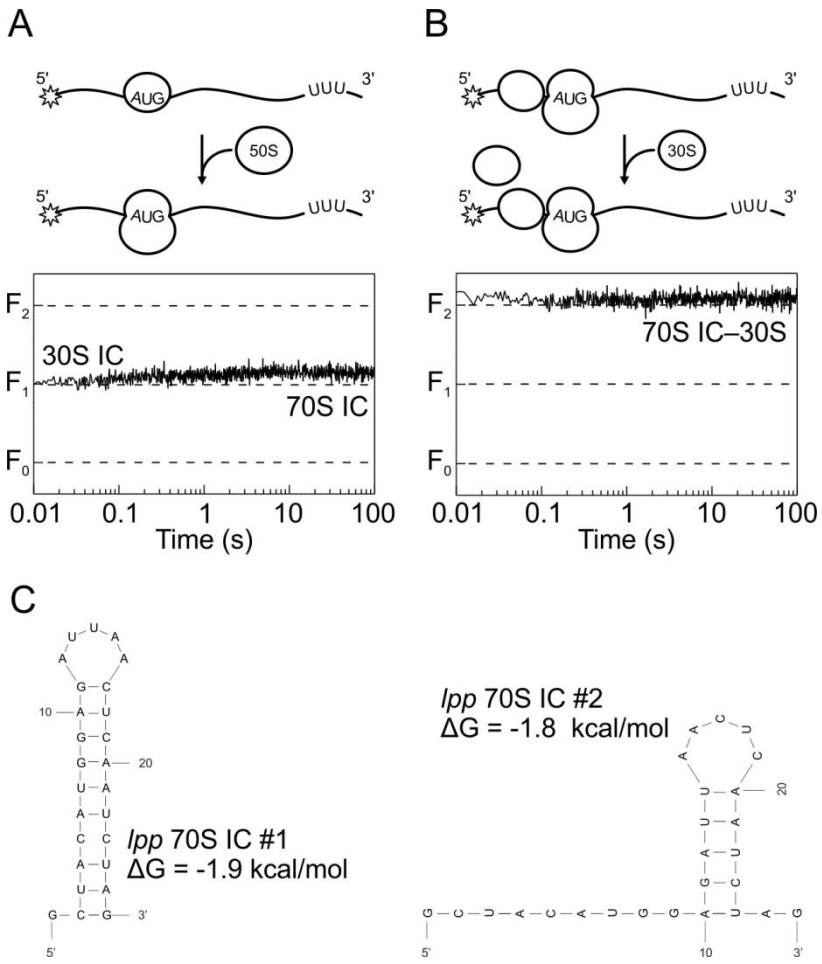

Fig. S3. Fluorescence of 5**lpp* **in different complexes.** (*A*) Lack of additional fluorescence change upon addition of the 50S subunits (0.05 μM) to the 30S IC prepared from 30S subunit (0.05 μM), IF1, IF2, IF3 (0.1 μM each), fMet-tRNA^{fMet} (0.15 μM), GTP (0.5 mM), and 5**lpp* mRNA (0.1 μM) for 20 min, 37°C. (*B*) Saturation of fluorescence change after the recruitment of a 30S PIC to the stand-by site. Purified 70S IC with 5**lpp* (0.05 μM) were incubated with the 30S IC (0.05 μM) for 1 min and subsequently mixed with excess of 30S PIC (0.3 μM). (*C*) Potential secondary structures in the *lpp* 5'UTR when the 70S IC occupies about 30 nt around the start codon.

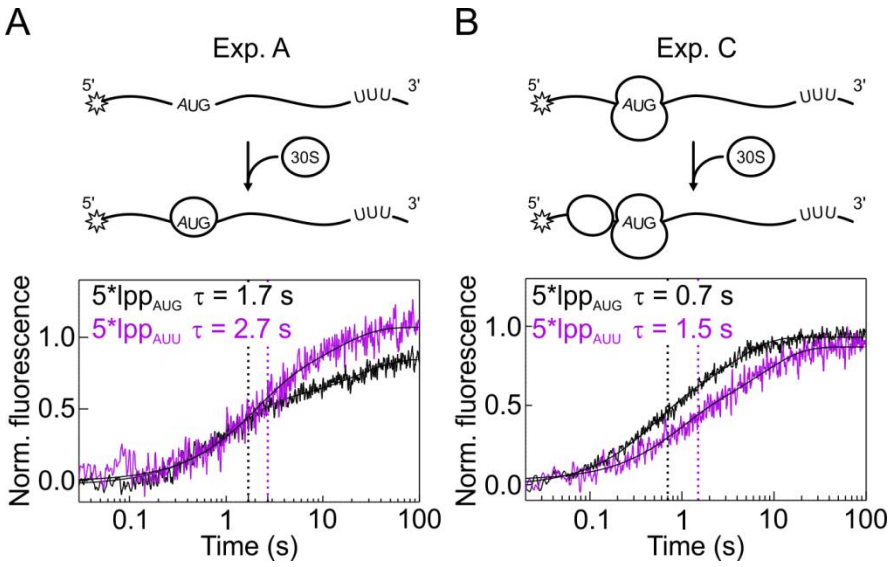

Fig. S4. 30S PIC recruitment to the stand-by site is independent of the AUG codon at the mRNA 5' end. (*A*) Fluorescence change of free 5**lpp* (black) and 5**lpp*$_{AUU}$ (purple) mRNAs (0.05 μM) upon mixing with the 30S PIC (0.15 μM). The fluorescence change was normalized taking into account the initiation efficiency of the respective mRNAs (Fig. S1*G*). Black lines represent two-exponential fits. The τ values are larger than in other Figures due to a lower 30S PIC concentration used in the experiment. (*B*) Recruitment of 30S PIC (0.3 μM) to the stand-by site on 5**lpp* (black) and 5**lpp*$_{AUU}$ (purple) mRNAs in complex with the 70S IC (0.05 μM).

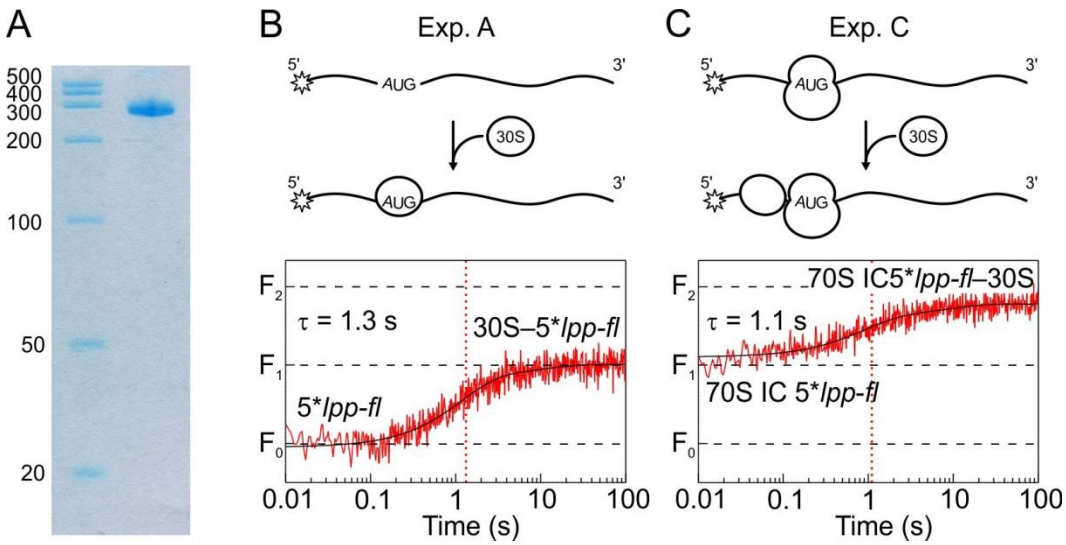

Fig. S5. **30S PIC recruitment to the stand-by site on the full-length lpp mRNA.** (*A*) Purity of the *lpp* mRNA analysed on the 8% urea PAGE and visualized by methylene blue staining. Left lane, commercial molecular weight marker (Dynamarker®RNA Low Easy Load; BioDynamics Laboratory Inc.); right lane, full-length *lpp* mRNA. (*B*) Fluorescence change of free 5**lpp-fl* mRNAs upon mixing with the 30S PIC. (*C*) Recruitment of 30S PIC to the stand-by site on 5**lpp-fl* mRNAs in complex with the 70S IC. Black lines represent two-exponential fits.

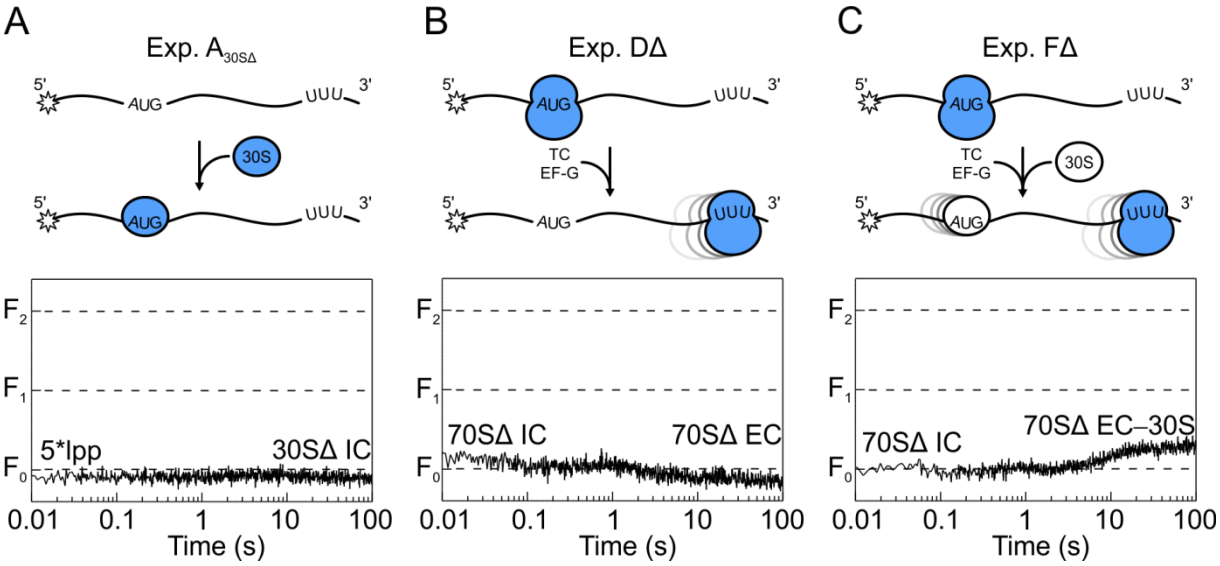

Fig. S6. Lack of 5**lpp* **fluorescence change upon interaction with ribosomes lacking proteins S1 and S2.** (*A*) Upon addition of 30SΔPIC. 5**lpp* mRNA (0.05 μM) was rapidly mixed with a complex formed of 30SΔ subunits (0.15 μM), IFs (0.3 μM each) and GTP (0.5 mM). Compare to Exp. A, Fig. 1B. (*B*) Upon translation by 70SΔ EC. Experimental conditions are as in Exp. D, Fig. 3. (*C*) Upon simultaneous addition of the elongation components and the 30S PIC, as in Exp. F in Fig. 3.

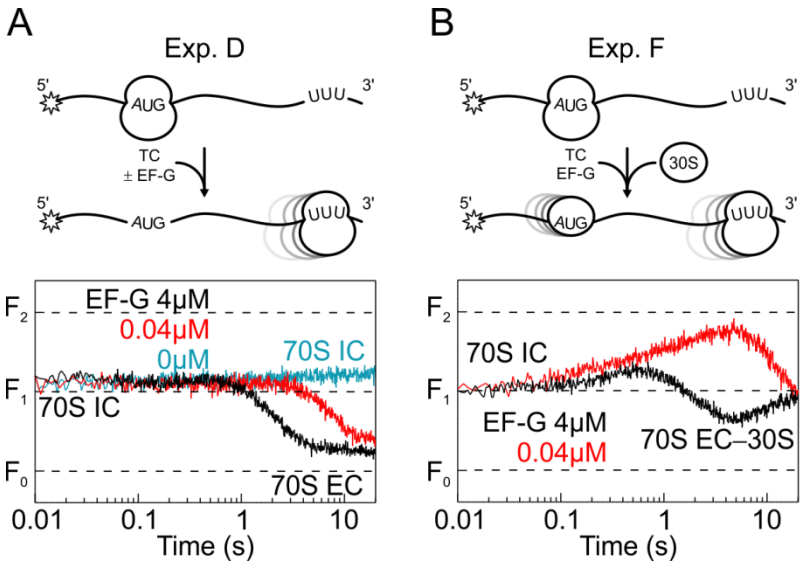

Fig. S7. Dependence of 5**lpp* **fluorescence changes on translation rate.** (*A*) Start codon clearance upon translation with different EF-G concentrations: saturating (4 μM; black trace), limiting (0.04 μM; red trace) or no EF-G (blue trace). (*B*) Translation with 30S PIC recruitment at saturating (4 μM; black trace) or limiting (0.04 μM; red trace) EF-G concentrations.

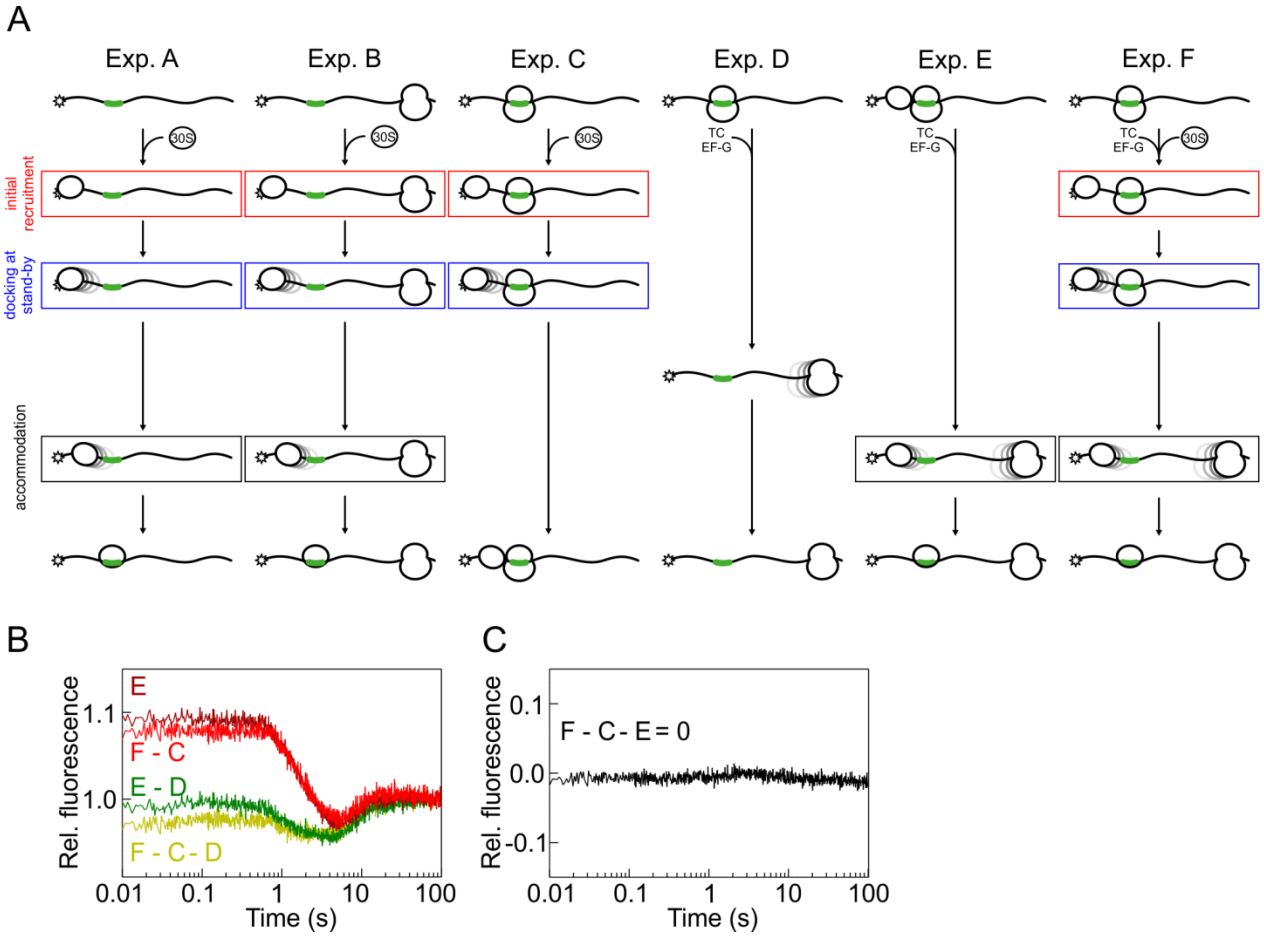

Fig. S8. Schematic of the processes that are probed in Exps. A-F and validation of the deconvolution strategy. (*A*) Depending on the experimental conditions, the following steps can occur. 30S PIC is recruited to the mRNA (step 1) and docks to the stand-by site (step 2). If the 30S is recruited to the free mRNA, the 30S subunit then finds the start codon and forms a stable 30S IC; however, the latter step is not reflected in a fluorescence change of 5**lpp* (Exp. A). A similar sequence of events is observed in the complex where the leading 70S EC has vacated the start codon as a result of translation (Exp. B). When 70S IC occupies the start codon, the next 30S PIC cannot read the start codon, but is till recruited to the stand-by site (Exp. C). Translation changes the 5**lpp* fluorescence (Exp. D). In the complex where two ribosomes are bound at the onset of elongation, translating 70S EC vacates the start codon, allowing the 30S PIC to move from the stand-by site to the start codon (Exp. E). Upon simultaneous addition of the elongation machinery and the 30S PIC, elongation and all steps resulting in the recruitment and accommodation of the second 30S subunit occur concomitantly (Exp. F). The difference between the schematics directly

shows how particular steps can be extracted by subtraction of the respective time courses from one another. (*B*) Comparison of the experimentally measured trace of Exp. E (dark red) (same trace as in Fig. 3) with the trace calculated by subtraction of Exp. C from Exp. F (light red), which should reflect the same processes as Exp. E, e.g., movement of the 70S EC away from the start codon and accommodation of the 30S subunit (*A*). Trace E-D reflects only the 30S IC accommodation at the start codon (green; see *A*) and the same step should appear upon subtraction of F-C-D (dark yellow), which is in fact the case. (*C*) Subtraction of F-C-E should cancel all signal changes (see *A*), which is confirmed here.

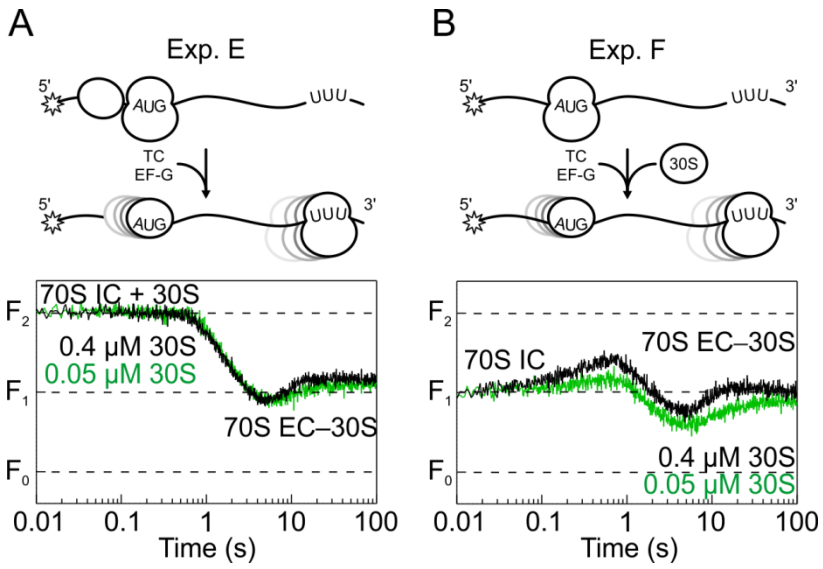

Fig. S9. Examples of time courses obtained at different 30S PIC concentrations and used in the global fit model. (*A*) Time courses of Exp. E (see also Fig. 3). Green trace, 0.05 µM 30S PIC, black trace, 0.4 µM 30S PIC. (*B*) Same as in (*A*) for Exp. F. (see also Fig. 3).

Table S1. List of oligonucleotides used to assemble the dual luciferase reporters.

Name	Sequence (5′ to 3′)
Fluc_F	ACAATAATGACCTCTAGAAATAATTTTGTTTAACTTTAAGAAG
Fluc_R	TTAGCAGCCGGATCTCATTACAATTTGGACTTTCCGCCC
pET_F	TAATGAGATCCGGCTGCTAACAAAGCCCGAAAGGAAGCTG
pET_R	TAGATTGAGTTAATCTCCATGTAGCTATAGTGAGTCGTATTAATTTCGCGG
pET_WR	ATGGTGACTCTAATCTTTCTCTAGACTATAGTGAGTCGTATTAATTTCGCGG
Rluc_F1	CAATCTAGAGGGTATTAATAATGACTTCGAAAGTTTATGATCCAG
Rluc_F	CTACATGGAGATTAACTCAATCTAGAGGGTATTAATAATGACTTCG
Rluc_R	ATTTCTAGAGGTCATTATTGTTCATTTTTGAGAACTCG
Rluc_WF	GTCTAGAGAAAGATTAGAGTCACCATATGACTTCGAAAGTTTATGATCCAG

SUPPLEMENTAL REFERENCES

1. Kosuri S, *et al.* (2013) Composability of regulatory sequences controlling transcription and translation in Escherichia coli. *Proc Natl Acad Sci U S A* 110:14024-14029.
2. Gibson DG, *et al.* (2009) Enzymatic assembly of DNA molecules up to several hundred kilobases. *Nat Methods* 6:343-345.
3. Gibson DG (2011) Enzymatic assembly of overlapping DNA fragments. *Methods Enzymol* 498:349-361.
4. Milon P, *et al.* (2007) Transient kinetics, fluorescence, and FRET in studies of initiation of translation in bacteria. *Methods Enzymol* 430:1-30.
5. Rodnina MV & Wintermeyer W (1995) GTP consumption of elongation factor Tu during translation of heteropolymeric mRNAs. *Proc Natl Acad Sci USA* 92:1945-1949.
6. Rodnina MV, *et al.* (1999) Thiostrepton inhibits the turnover but not the GTPase of elongation factor G on the ribosome. *Proc Natl Acad Sci USA* 96:9586-9590.
7. Wieden HJ, Gromadski K, Rodnin D, & Rodnina MV (2002) Mechanism of elongation factor (EF)-Ts-catalyzed nucleotide exchange in EF-Tu. Contribution of contacts at the guanine base. *J Biol Chem* 277:6032-6036.
8. Rodnina M (1994) Purification of fMet-tRNA^{fMet} by Fast Protein Liquid Chromatography. *Anal Biochem* 219:380-381.
9. Gromadski KB, Wieden HJ, & Rodnina MV (2002) Kinetic mechanism of elongation factor Ts-catalyzed nucleotide exchange in elongation factor Tu. *Biochemistry* 41:162-169.
10. Posfai G, *et al.* (2006) Emergent properties of reduced-genome Escherichia coli. *Science* 312:1044-1046.
11. Bollen A, *et al.* (1979) A conditionally lethal mutation of Escherichia coli affecting the gene coding for ribosomal protein S2 (rpsB). *J Mol Biol* 132:219-233.
12. Link AJ, Phillips D, & Church GM (1997) Methods for generating precise deletions and insertions in the genome of wild-type Escherichia coli: application to open reading frame characterization. *J Bacteriol* 179:6228-6237.
13. Powers T & Noller HF (1991) A functional pseudoknot in 16S ribosomal RNA. *EMBO J* 10:2203-2214.
14. Davydov, II, *et al.* (2013) Evolution of the protein stoichiometry in the L12 stalk of bacterial and organellar ribosomes. *Nat Commun* 4:1387.

15. Cox J*, et al.* (2014) Accurate proteome-wide label-free quantification by delayed normalization and maximal peptide ratio extraction, termed MaxLFQ. *Mol Cell Proteomics* 13:2513-2526.
16. Bernasconi CF (1976) *Relaxation Kinetics* (Academic press, New York, San Francisco, London) p 289.
17. Johnson KA (2009) Fitting enzyme kinetic data with KinTek Global Kinetic Explorer. *Methods Enzymol* 467:601-626.
18. Zuker M (2003) Mfold web server for nucleic acid folding and hybridization prediction. *Nucleic Acids Res* 31:3406-3415.